

# Multi Loss Fusion For Matching Smartphone Captured Contactless Finger Images

Bhavin Jawade, Akshay Agarwal, Srirangaraj Setlur, Nalini Rath

Computer Science and Engineering

University at Buffalo, USA

{bhavinja, aa298, setlur, nratha}@buffalo.edu

**Abstract**—Traditional fingerprint authentication requires the acquisition of data through touch-based specialized sensors. However, due to many hygienic concerns including the global spread of the COVID virus through contact with a surface has led to an increased interest in contactless fingerprint image acquisition methods. Matching fingerprints acquired using contactless imaging against contact-based images brings up the problem of performing cross modal fingerprint matching for identity verification. In this paper, we propose a cost-effective, highly accurate and secure end-to-end contactless fingerprint recognition solution. The proposed framework first segments the finger region from an image scan of the hand using a mobile phone camera. For this purpose, we developed a cross-platform mobile application for fingerprint enrollment, verification, and authentication keeping security, robustness, and accessibility in mind. The segmented finger images go through fingerprint enhancement to highlight discriminative ridge-based features. A novel deep convolutional network is proposed to learn a representation from the enhanced images based on the optimization of various losses. The proposed algorithms for each stage are evaluated on multiple publicly available contactless databases. Our matching accuracy and the associated security employed in the system establishes the strength of the proposed solution framework.

## I. INTRODUCTION

Fingerprints are the oldest and most widely used biometric modality and fingerprint based systems are typically the most accurate biometric authentication systems. The two most important downsides of using fingerprints are hygiene and physical sensor disadvantage [1]. Using a contact-based sensor at border crossings can elevate the risk of spreading infectious bacteria and viruses. In particular, current COVID-19 pandemic has caused us to rethink users interaction with biometrics devices. Moreover, the need for biometric authentication in remote areas is increasing in various fields where expensive fingerprint scanners are difficult to be deployed. It has been reported that more than 1.1 billion vaccinated users in remote areas of Asia and Africa that are not enrolled in any biometric database [18]. Therefore, there is a need for portable, low-cost, and easy-to-use fingerprint enrollment and verification solutions that rely on commercial grade user owned devices such as mobile phones or tablets. Additionally, smartphone-based fingerprint enrollment can save users from the hassle of going to a biometric enrollment agency and can also lead to faster processing at airports and border crossings. Capturing a user's fingerprint using their smartphone's camera and then performing fingerprint matching at a secure server against a

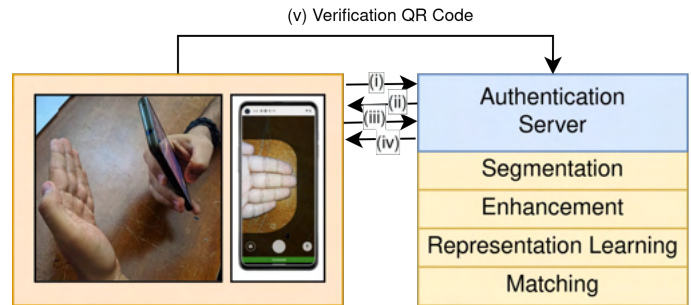


Fig. 1: System architecture: (i) the client sends a transaction request to the server (ii) the server responds with a steganographic challenge. (iii) application hides the steganographic challenge within the captured image and sends the encrypted packet back to the server. (iv) After verifying the challenge data, the server segments the four-finger region and the distal phalange from the image, enhances the fingerprint, extracts the representation, matches the representation against the template representation stored in the database, and if it matches responds with the verification QR code. (v) User can scan the QR code displayed on the screen at the access granting agency, which can verify the QR code with the authentication server.

legacy contact-based or newly acquired touchless fingerprint database could provide an effective alternative to overcome these limitations of contact-based fingerprints. Other benefits of contactless fingerprint image acquisition are the easy availability of low-cost mobile sensors, improved hygiene, and avoidance of sensor getting dirty due to continuous touch.

Designing a contactless matching system requires special considerations to be given to security, ease-of-use, fingerprint quality, and matching robustness. NIST [10] provides general guidelines for contactless fingerprint acquisition and also lists various challenges presented by image anomalies. Some of the common challenges of a contactless fingerprint system are (i) polarity conversion - depending upon the angle of illumination a decision has to be made about which feature has to be considered as a ridge or a furrow while grayscaling, (ii) poor focus - portions of the fingerprint region which are out of the depth of field of the camera are usually blurred causing loss of important discriminative information, (iii) finger angle - variations in the finger angle along the yaw, pitch, and roll axes due to the unconstrained nature of contactless fingerprint acquisition, and (iv) skin irregularities - effects of skin

irregularities such as grooves and scars could be intensified when working with a contactless fingerprint. In addition to overcoming these challenges, an important factor to keep in mind while designing a contactless fingerprint system is cross-sensor compatibility with existing contact-based fingerprints.

The key contributions of this research are:

- 1) An end-to-end system design capable of enrolling, verifying, and authenticating a user using contactless fingerprints acquired using their smartphone.
- 2) A cross-platform mobile application that can be directly operated by the user for acquiring photos of the four-finger region.
- 3) A novel amalgamation of grabcut and HSV thresholding for fast and efficient segmentation of finger region.
- 4) A multi-step contactless fingerprint enhancement pipeline that overcomes various challenges of extracting ridge patterns from contactless fingerprint images acquired using a smartphone.
- 5) A novel score level fusion of deep metric AdaCos Loss with a Contrastive Loss network utilizing weak supervision from handcrafted minutiae features for contactless fingerprint matching that achieves results on par or better than existing deep networks.

Various steps in our proposed solution is shown in Fig. 1

## II. RELATED WORK

Current methods of contact-based fingerprint acquisition suffers from various limitations including latent fingerprints left on sensor platen, distortions caused due to flattening of the skin against the surface, and image differences caused due to variations in moisture level and pressure at fingertip [9]. Fig. 2 shows some of the potential drawbacks of contact-based fingerprint systems. Due to these reasons, fingerprint recognition needs to focus on contactless methods over contact-based images. However, the image acquisition from user mobile device based cameras need to address distortions such as motion blur, resolution, and image quality. A typical fingerprint recognition pipeline consists of the following steps: (i) segmentation, i.e., extraction of the region of interest, (ii) image enhancement to overcome the distortions, and (iii) representation learning and (iv) matching.

Given the large background area captured in finger-selfies or contactless images, segmentation of the finger region is a critical step. Malhotra et al. [14] proposed segmentation of the finger region using a combination of masks obtained using the saliency map and skin color. It is noted in the work that the segmentation fails in the presence of complex backgrounds and high illumination. To counter such limitations, Grosz et al. [5] have proposed a U-Net autoencoder architecture. After segmentation, image enhancement is an important step. Lin et al. [13] and Grosz et al. [5] have applied adaptive histogram equalization and contrast adjustment for image enhancement. But contactless and contact-based images suffer from distortions for different reasons. Hence, several distortion correction methods have been proposed in the literature to improve the quality of fingerprint images. Lin and Kumar [11] have



Fig. 2: Drawbacks of contact-based fingerprints. (i) Fingerprint scanners at Airport Terminals, bank ATMs, etc increase the risk of touch-based COVID infection. (ii) Latent fingerprints from public fingerprint scanners can be used to recreate fingerprint spoofs for presentation attacks.

proposed an algorithm to counter the non-linear deformations present in a contact-based image. Li et al. [13] have proposed a generalized distortion correction model based on a robust thin-spline plate model. Once the region of interest is extracted and modified for matching through enhancement, the final step is to apply machine learning algorithms for matching. The matching consists of two stages: (i) feature extraction and (ii) classification. Fingerprint matching approaches in the literature can be broadly categorized into two classes, those based on minutiae or on deep learning features. Lin and Kumar [12] have used the Siamese architecture [3] for contactless to contact-based fingerprint matching. The authors have utilized the ridge map and minutiae map computed from both sensor-based and contactless-based fingerprint images. Malhotra et al. [14] have extracted the features from a deep scattering network [2] preserving multi-orientation and multi-scale information. Fingerprint verification is performed using random decision forests to classify the images as match or non-match. Grosz et al. [5] have utilized the score fusion between DeepPrint architecture trained on large public and private datasets [4] and the Verifinger commercial-off-the-shelf (COTS) system. The limitation of training on large privately available datasets is increased difficulty in reproducibility and comparison of results [19].

## III. PROPOSED FINGERPRINT MATCHING SYSTEM

### A. System Architecture

In this paper, we propose an end-to-end system for person authentication using contactless fingerprints. Details of the fingerprint acquisition app, the challenge-response method for secure transfer, finger region segmentation algorithm, finger print image enhancement, and representation learning are presented in this section. Fig. 1 shows the various components of the system and how data flows between them.

1) *Cross-Platform Mobile Application*: For acquiring fingerprints using a smartphone, a cross-platform mobile application has been developed using react-native<sup>1</sup>. After a user logs in to the application a bounded region is shown as a guide to place their hand after which the application runs the

<sup>1</sup><https://reactnative.dev/>

continuous autofocus to search for the right depth of field. It then captures a snapshot and records a 5-second continuous video that could be used for best frame and liveness detection. The same procedure is repeated for the other hand.

2) *Challenge-response*: To securely transfer the image to the server and to ensure that the image has not been tampered with, we implement a steganographic challenge-response mechanism. Upon receiving the request from the client, the server generates a random number  $N$  – (*Seed Initializer*) and a challenge message  $M$  of length  $n$  that will be sent back to the client in an asymmetrically encrypted packet. Then, both the server and the client use  $N$  to generate seed  $S$  using the following equation:

$$S = N \oplus K$$

Where  $\oplus$  denotes XOR operation and  $K$  is the shared key between the server and the client. Using the seed  $S$  and a pseudo-random number generator  $R$  both the server and the client generate a sequence of length  $n$  that denotes the locations of pixels on the image. Then the client performs LSB-based steganography over the  $n$  pixels in the image by hiding the message  $M$ . LSB steganography is performed by manipulating the least significant bit of each pixel value with the respective bit in the binary message. This steganographic image is sent back to the server, where the server uses the seed initializer, the shared key, and the pseudo-random number generator to get pixel locations. By matching the message retrieved from the image against the challenge message  $M$ , the server can ensure image integrity.

### B. Segmentation

To extract the finger region, an image is downsampled to 6% of its original size. This helps in speeding up the segmentation process. For the initial foreground mask required by the segmentation algorithm, we use the downsampled version of the guiding box presented in the app. Grabcut algorithm [16] is applied over the downsampled image to get the first mask  $M_g$ . This mask is applied over the captured image to get the segmented image. The segmented image is then converted from RGB to HSV for skin color thresholding using hue values in the range (0, 50) and saturation values in the range (0.23, 0.68) [15]. Morphological closing is then applied over the resultant skin mask to fill out small holes and aberrations. Next, we upscale both the skin segmented mask  $M_s$  and the grab cut mask  $M_g$  to the original size. Connected components search is performed over the two binary masks to get the largest components within the masks assuming that the hand region will be the largest component. After this, the two masks are multiplied to get the final mask  $M$  and we apply median blur on it to smoothen the pixelated edges caused by upscaling. Finally, we apply the mask over the original image  $I$  to segment the finger region. Throughout these steps, only masks are up-scaled thereby ensuring no loss in image quality.

Fig. 3<sup>2</sup> shows the comparison of the proposed approach over just using the skin segmentation or grabcut. To extract the dis-

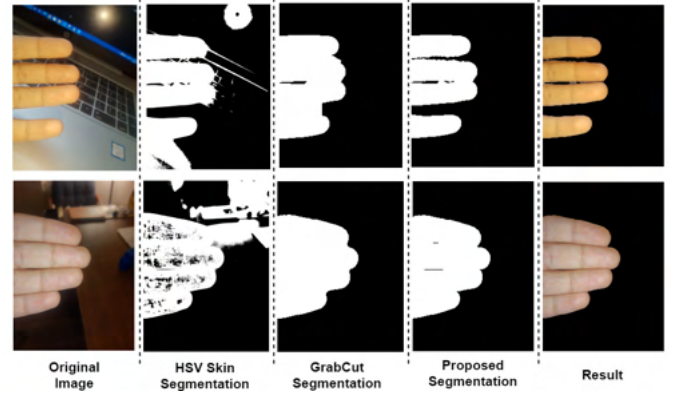


Fig. 3: Effects of using either HSV color space skin segmentation or GrabCut alone against our proposed method.

tal phalanges from the finger region we train a MaskRCNN [7] on 380 manually labeled images from the IIIT-D Smartphone Finger-selfie Database v2 [17].

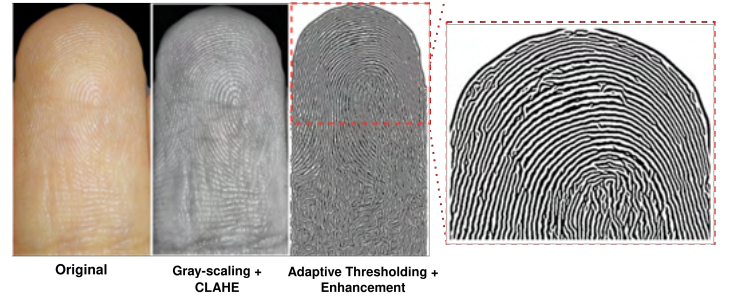


Fig. 4: Various steps involved in extracting the ridge patterns from the contactless fingerprint image.

### C. Fingerprint Image Enhancement

There is a significant domain gap between the contactless and contact-based images and also between contactless images acquired in different lighting conditions or with different sensors. To compensate for this domain gap and extract a better quality ridge pattern from the contactless images, we perform various enhancement steps on the segmented images of the existing databases. The segmented region is first preprocessed by applying the adaptive histogram equalization to improve the local contrast and redistribute the lightness values of the image. Later, image sharpening is applied by subtracting the Gaussian blurred image from it. In the end, adaptive mean thresholding is adopted to binarize the image.

Once we have the ridges extracted from an enhanced image, directional median filtering [21] is utilized to further improve the image quality. In this method, an image is first convolved with an anisotropic kernel and then filtered using a directional median filter. The anisotropic filter uses a kernel with a shape adapted specifically for local intensity orientation in a fingerprint image. The generalized form of an anisotropic filter is given as:

$$H(x_0, x) = V + S\rho(x - x_0)\exp(N)$$

<sup>2</sup>Illustrations in Fig. 3 and 4 use sample images captured using our new contactless image acquisition app.



$$N = - \left[ \frac{((x - x_0) \cdot n)^2}{\sigma_1^2(x_0)} + \frac{((x - x_0) \cdot n_\perp)^2}{\sigma_2^2(x_0)} \right]$$

Here  $V$  and  $S$  control the phase intensity and impact of the neighborhood and  $\sigma_1^2(x_0)$  and  $\sigma_2^2(x_0)$  control the shape of the filter kernel. As described in the paper we use  $V = -2$  and  $S = 10$  in the implementation.  $n$  is the unit vector along the direction of the ridge line. Fig. 4 shows the various stages of image preprocessing and fingerprint enhancement.

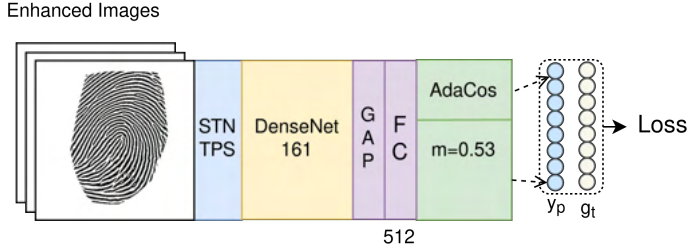


Fig. 5: Deep network trained using adaptive scaling cosine loss.

#### D. Representation Learning

Learning a fixed-length embedding is a well-studied problem in the domain of deep metric learning and has shown success in applications such as face recognition and person re-identification. Due to the various challenges described earlier, extracting a good minutiae map from a contactless fingerprint is difficult. Therefore, we propose two different network architectures, one that minimizes a deep metric loss to learn discriminative features and another that uses a contrastive loss between pairs of images along with a minutiae loss branch to reconstruct minutiae maps.

Angular margin losses or cosine margin losses have shown success in tasks such as face recognition. With this motivation, we employ an Adaptive cosine scaling loss (AdaCos) [22] to learn fixed-length embeddings from the enhanced fingerprint images. Fig. 5 shows the architecture of the AdaCos pipeline. One of the challenges of earlier cosine margin losses is difficulty in hyperparameter tuning. AdaCos solves this by setting the initial hypersphere scale parameter as:

$$s = \sqrt{2} * \log(N - 1)$$

where  $N$  is the number of classes in the training set. We set the margin empirically as 0.53. Embeddings and the weights are normalized before computing AdaCos scaled features. The scale parameter is recomputed in each step using the following equation:

$$s_d^{(t)} = \frac{\log B_{avg}^{(t)}}{\cos(\min(\frac{\pi}{4}, \theta_{med}^{(t)}))} [22]$$

where  $B_{avg}^{(t)}$  is the dynamic scale parameter computed using the scale from the previous iteration. The distance metric used to compare the embeddings in the AdaCos network is the cosine similarity. In our experiments, we found that training angular margin losses is difficult with a small amount of

data as it leads to overfitting and lower generalization. To overcome this challenge, we pre-train our AdaCos network on 0.1M synthetically generated fingerprint images created using the Anguli Fingerprint generator<sup>3</sup>. Further data augmentation is performed using on-the-fly strategies that include random perspective distortion, random gaussian blurring, and resized cropping. Then we fine-tune the pre-trained network on the PolyU dataset and ISPF v1 and v2 datasets for the respective experiments.

In addition to the AdaCos Network, we train a contrastive network with minutiae reconstruction loss. Fig. 6 shows the pipeline for learning contrastive representation for the contactless to contact-based matching task. The network is trained in Siamese setting with shared weights, taking as input two enhanced fingerprint images resized to (224, 224), and passing them through a spatial transformer network (STN) [8] which uses a thin plate spline transformation. Fingerprint images transformed using STN are then passed through the convolutional layers of a DenseNet 161 feature extractor (initialized with pre-trained ImageNet weights) to learn downscaled tensors. From here the network divides into three parts: (i) Minutiae branch for the contactless image (ii) Minutiae branch for the contact-based image (iii) Contrastive branch to learn discriminative features from the images.

For the contrastive branch, we first perform 2D average pooling on the two downscaled tensors and flatten them to get one-dimensional representations. Then we pass these 1D representations through fully connected layers to learn fixed-length embeddings of size 512. Next, we calculate the euclidean distance between these two embeddings and compute the double margin contrastive loss [6]. The formulation for double margin contrastive loss is given as:

$$L_{con}(I_{cl}, I_{cb}) = \frac{1}{2} [y \cdot (d - \alpha_1)^2 + (1 - y) \max(\alpha_2 - d, 0)^2]$$

Here,  $\alpha_1$  and  $\alpha_2$  denote the margins for the positive and negative pairs respectively.  $d$  is the distance metric which in this case is euclidean distance. After empirically experimenting with the two margins and observing the histogram of the distance between positive and negative pairs, we select  $\alpha_1$  as 0.92 and  $\alpha_2$  as 3.20. Using just the contrastive loss leads to slower training and overfitting. To overcome this, we compute the minutiae loss for the two images which helps the network learn minutiae-like features and generalize to the unseen images where minutiae might not be available. For this, we upscale the output tensors from the DenseNet161 backbone to the original size using deconvolutional layers. Then we compute the pixel-wise cross-entropy loss between the upscaled tensors and the ground truth minutiae maps extracted from NIST's mindtct minutiae extractor. Let  $L_{CB}$  and  $L_{CL}$  be the minutiae loss for the contactless and contact-based images, then the final loss function is given by the weighted sum of the three losses:

$$L = \beta \cdot L_{CB} + \beta \cdot L_{CL} + L_{con}$$

<sup>3</sup><https://dsl.cds.iisc.ac.in/projects/Anguli/>

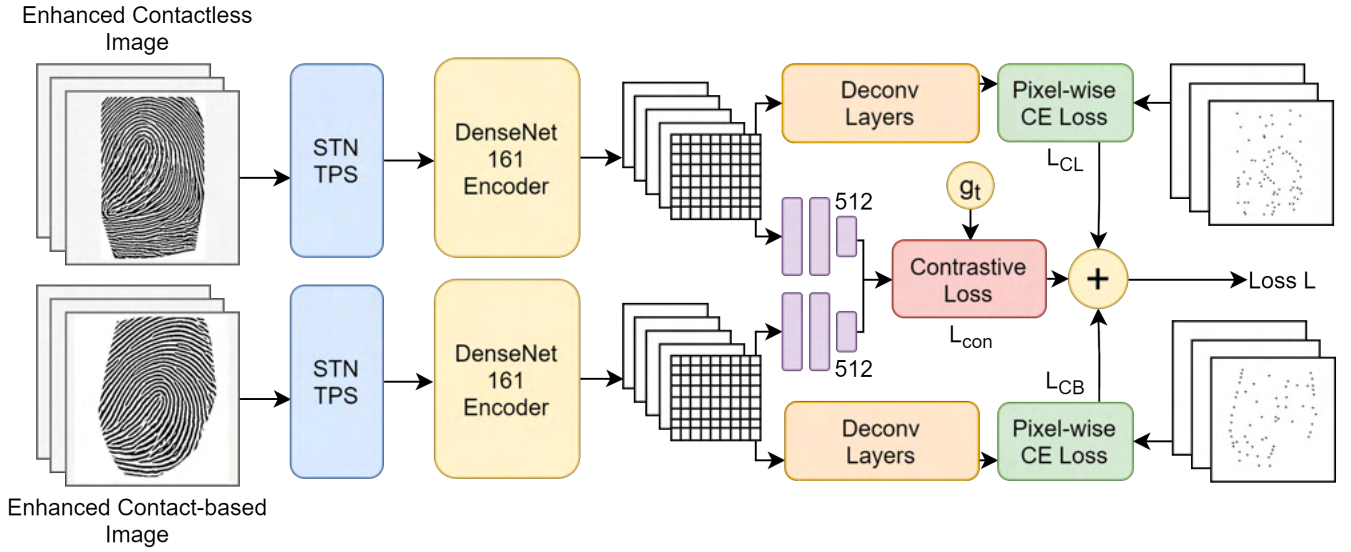


Fig. 6: Contrastive learning network with minutiae reconstruction loss

TABLE I: Comparison with COTS, Multi-Siamese [12], and Minutiae Attention Network (MANet) [20] on the PolyU dataset

Metric	COTS	MANet	Multi-Siamese	Proposed		
				Minutiae + Contrastive	AdaCos	Fusion
EER (%)	6.10	4.13	7.11	4.18	5.28	<b>4.07</b>
TAR (%) @FAR= $10^{-3}$	82.5	68.5	44.0	<b>70.2</b>	61.5	<b>72.3</b>
TAR (%) @FAR= $10^{-2}$	89.3	85.0	68.0	<b>92.5</b>	<b>88.5</b>	<b>94.4</b>

TABLE II: EER (%) comparison of proposed network with COTS, DSN-RDF [14] on the ISFPDv2, ISFPDv1

Dataset	COTS	DSN-RDF	Proposed
ISFPDv1	39.52*	5.53-7.07 [17]	<b>3.12</b>
ISFPDv2	12.03*	<b>3.41</b> [14]	4.20

\*We observed that for more than 50% of the images, Verifinger couldn't enroll due to zero minutiae count. A similar observation has been made by [14] for NFIS

TABLE III: Ablation Study on our proposed method.

Ablation Setting					Metric
$E_p$	$E_c$	$T_s$	$M_l$	$A$	EER (%)
✓					18.4
✓	✓				7.98
✓	✓	✓			6.43
✓	✓	✓	✓		5.01
✓	✓	✓	✓	✓	4.18

$E_p$  - Preprocessing,  $E_c$  - Chaohong et.al Enhancement Method,  $T_s$  - Spatial Transformer Network,  $M_l$  - Minutiae Loss Branch,  $A$  - On the fly augmentations

Here weight  $\beta$  was set empirically. To compensate for the small dataset, training was done using on-the-fly image transformations which included random rotations and resized random cropping. Each training batch (size 32) consisted of an equal number of randomly mined positive and negative pairs.

#### IV. RESULTS AND ANALYSIS

The model is evaluated on the PolyU dataset [13] and ISFPD v1 and v2 datasets [14], [17]. Table I shows the comparison of our representation learning architecture with the directly reported results in the respective papers. For contactless to contact-based comparison on ISFPD dataset,

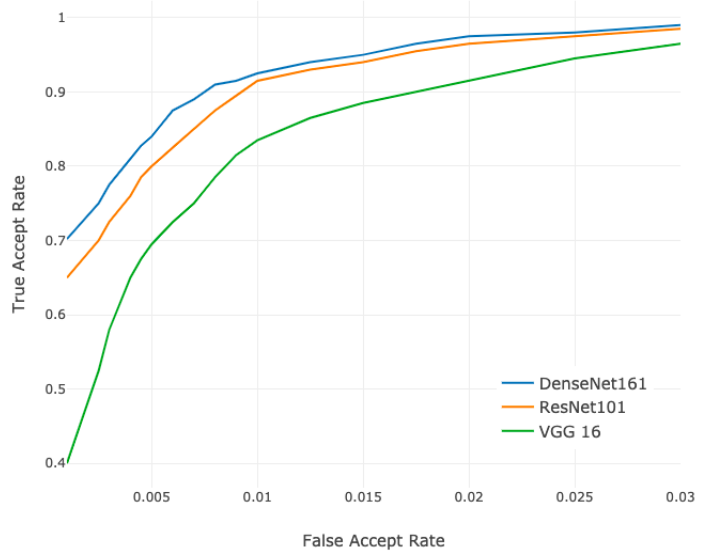


Fig. 7: ROC curve for the proposed method with different conv-net backbones.

we compute results on White Indoor Vs Live Scan with 50% test-train split. We also compare our results against a COTS fingerprint matcher (Verifinger SDK 12.0). It can be observed that using contrastive loss with minutiae branch alone gives a substantial improvement of 3% EER over the Multi-Siamese CNN [12] and performs on par with MANet [20]. We observed that even though the AdaCos Network does not have a minutiae reconstruction branch, it is still able to

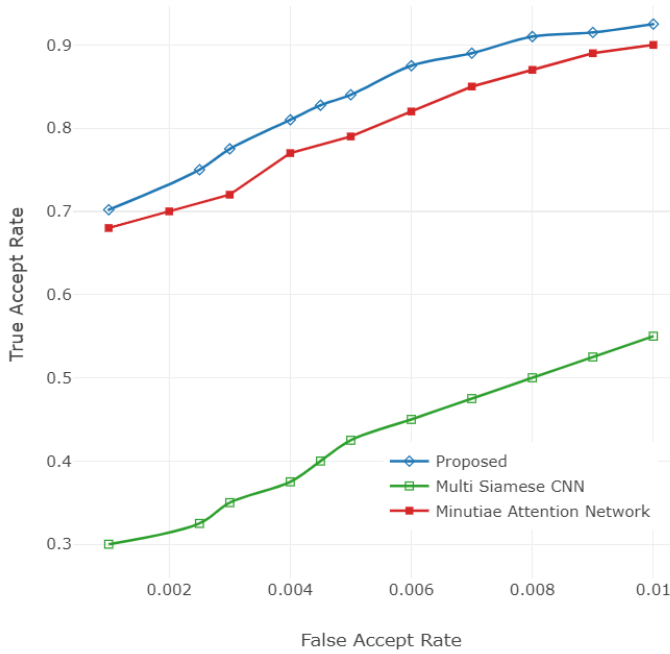


Fig. 8: ROC curve of the proposed method, Multi-Siamese CNN (Lin et.al [12]) and Minutiae Attention Network [20].

learn discriminative features and has a lower equal error rate (EER) than the Multi-Siamese CNN [12]. Finally, performing a score level fusion by normalizing the similarity scores from the two networks further lowers the EER and increases the TAR. Fig. 8 shows the ROC comparison of different matching algorithms. It can be observed that the proposed algorithm outperforms the existing deep learning methods, and achieves results close to the COTS Verifinger matcher. Table II shows the evaluation of the proposed pipeline on the ISFPD dataset. The proposed algorithm surpasses the commercial system by a significant margin. The proposed algorithm outperforms the current state-of-the-art algorithm [17] on the ISFPDv1 database, and performs comparably [14] on ISFPDv2.

Table III shows the ablation study of the various components of the representation learning pipeline. As can be observed, just using the enhancement procedure results in a significant drop in equal error rate without even using minutiae loss or transforming images using a spatial transformer network. Using the STN-TPS block along with the minutiae branch further boosts the matching performance. Fig. 7 shows the comparison of different backbone architectures for the contrastive network with minutiae loss.

## V. CONCLUSION

In this research, we have proposed effective algorithms for contactless fingerprint matching covering region extraction, image enhancement, and matching. A grab cut algorithm is proposed for the segmentation of fingerprint regions to improve the performance compared to existing algorithms. For matching, a two-way architecture is proposed based on the minimization of the various loss functions. The proposed multi-branch network surpasses existing algorithms including

commercial systems on multiple challenging databases such as PolyU and ISFPD. We have developed a mobile application with an end-to-end pipeline ranging from data acquisition to fingerprint matching for contactless person authentication. We strongly believe that our end-to-end system design will help promote widespread adoption of smartphone-based contactless fingerprint authentication. In turn, this can help alleviate the risk of virus transmission and other drawbacks of traditional contact-based fingerprint biometric enrollment.

## ACKNOWLEDGMENT

This work was conducted at the Center for Unified Biometrics and Sensors (CUBS) at the University at Buffalo and was supported by the Center for Identification Technology Research (CITeR) and the National Science Foundation through grant #1822190.

## REFERENCES

- [1] Facial recognition vs. fingerprint recognition - what biometric is better. <https://recfaces.com/articles/facial-vs-fingerprints-biometrics>, Nov 2020.
- [2] Joan Bruna and Stéphane Mallat. Invariant scattering convolution networks. *IEEE TPAMI*, 35(8):1872–1886, 2013.
- [3] Sumit Chopra, Raia Hadsell, and Yann LeCun. Learning a similarity metric discriminatively, with application to face verification. In *IEEE CVPR*, volume 1, pages 539–546, 2005.
- [4] Joshua James Engelsma, Kai Cao, and Anil K Jain. Learning a fixed-length fingerprint representation. *IEEE TPAMI*, 2019.
- [5] Steven A Grosz, Joshua J Engelsma, and Anil K Jain. C2cl: Contact to contactless fingerprint matching. *arXiv preprint arXiv:2104.02811*, 2021.
- [6] Jiedong Hao, Jing Dong, Wei Wang, and Tieniu Tan. Deepfirearm: Learning discriminative feature representation for fine-grained firearm retrieval, 2018.
- [7] Kaiming He, Georgia Gkioxari, Piotr Dollár, and Ross Girshick. Mask r-cnn. In *IEEE ICCV*, pages 2961–2969, 2017.
- [8] Max Jaderberg, Karen Simonyan, Andrew Zisserman, and Koray Kavukcuoglu. Spatial transformer networks, 2016.
- [9] Ruggero Donida Labati, Angelo Genovese, Vincenzo Piuri, and Fabio Scotti. Contactless fingerprint recognition: A neural approach for perspective and rotation effects reduction. In *2013 IEEE Symposium on Computational Intelligence in Biometrics and Identity Management (CIBIM)*, pages 22–30, 2013.
- [10] John Libert, John Grantham, Bruce Bandini, Stephen Wood, Michael Garriss, Kenneth Ko, Frederick Byers, and Craig Watson. Guidance for evaluating contactless fingerprint acquisition devices, 2018-07-27 2018.
- [11] Chenhao Lin and Ajay Kumar. Improving cross sensor interoperability for fingerprint identification. In *IEEE ICPR*, pages 943–948, 2016.
- [12] Chenhao Lin and Ajay Kumar. A cnn-based framework for comparison of contactless to contact-based fingerprints. *IEEE TIFS*, 14(3):662–676, 2018.
- [13] Chenhao Lin and Ajay Kumar. Matching contactless and contact-based conventional fingerprint images for biometrics identification. *IEEE TIP*, 27(4):2008–2021, 2018.
- [14] Aakarsh Malhotra, Anush Sankaran, Mayank Vatsa, and Richa Singh. On matching finger-selfies using deep scattering networks. *IEEE TBIOIM*, 2(4):350–362, 2020.
- [15] V. A. Oliveira and A. Conci. Skin detection using hsv color space. 2009.
- [16] Carsten Rother, Vladimir Kolmogorov, and Andrew Blake. "grabcut": Interactive foreground extraction using iterated graph cuts. In *ACM SIGGRAPH 2004 Papers*, page 309–314, 2004.
- [17] Anush Sankaran, Aakarsh Malhotra, Apoorva Mittal, Mayank Vatsa, and Richa Singh. On smartphone camera based fingerphoto authentication. In *IEEE BTAS*, pages 1–7, 2015.
- [18] Samanth Subramanian. <https://www.bloomberg.com/features/2020-covid-vaccine-tracking-biometric/>, august 2020.
- [19] Ai Takahashi, Yoshinori Koda, Koichi Ito, and T. Aoki. Fingerprint feature extraction by combining texture, minutiae, and frequency spectrum using multi-task cnn. *IEEE ICB*, pages 1–8, 2020.
- [20] Hanzhuo Tan and Ajay Kumar. Minutiae attention network with reciprocal distance loss for contactless to contact-based fingerprint identification. *IEEE TIFS*, 16:3299–3311, 2021.
- [21] Chaohong Wu, Zhixin Shi, and Venu Govindaraju. Fingerprint image enhancement method using directional median filter. In Anil K. Jain and Nalini K. Ratha, editors, *Biometric Technology for Human Identification*, volume 5404 of *Society of Photo-Optical Instrumentation Engineers (SPIE) Conference Series*, pages 66–75, August 2004.
- [22] Xiao Zhang, Rui Zhao, Yu Qiao, Xiaogang Wang, and Hongsheng Li. Adacos: Adaptively scaling cosine logits for effectively learning deep face representations. *CoRR*, abs/1905.00292, 2019.